

Received: 2020.10.17  
Accepted: 2020.12.03  
Available online: 2021.04.19  
Published: 2021.08.04

# Se-Methylselenocysteine Alleviates Liver Injury in Diethylnitrosamine (DEN)-Induced Hepatocellular Carcinoma Rat Model by Reducing Liver Enzymes, Inhibiting Angiogenesis, and Suppressing Nitric Oxide (NO)/Nitric Oxide Synthase (NOS) Signaling Pathway

Authors' Contribution:  
Study Design A  
Data Collection B  
Statistical Analysis C  
Data Interpretation D  
Manuscript Preparation E  
Literature Search F  
Funds Collection G

ABCDEF 1 **Jun Ding\***  
BCDEF 2 **Chuang Qi\***  
BCDF 1 **Jinmao Li**  
BCD 2 **Chuying Huang**  
BCF 1 **Jiayao Zhang**  
BC 1 **Yong Zhang**  
BCF 1 **Yi Li**  
CF 1 **Bin Fan**

1 Department of Hepatobiliary Surgery, The Central Hospital of Enshi Tujia and Miao Autonomous Prefecture, Enshi, Hubei, PR China  
2 Department of Oncology, The Central Hospital of Enshi Tujia and Miao Autonomous Prefecture, Enshi, Hubei, PR China

\* Jun Ding and Chuang Qi contributed equally to this study and are co-first author

**Corresponding Author:** Jun Ding, e-mail: [dingjun845@163.com](mailto:dingjun845@163.com)

**Source of support:** This study was supported by Enshi Tujia And Miao Autonomous Prefecture Science and Technology Project (Grant No. E20170006)

**Background:** Hepatocellular carcinoma is the third leading cause of cancer-associated mortality. This study aimed to investigate the effects of se-methylselenocysteine (MSC) on oncogenesis of diethylnitrosamine (DEN)-induced hepatocellular carcinoma.

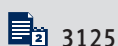
**Material/Methods:** A hepatocellular carcinoma rat model was established by administering DEN. Rat models were divided into Model (0.1 mg/kg MSC), Model+0.3 mg/kg MSC, Model+1 mg/kg MSC, and Model+3 mg/kg MSC groups. A Normal control group consisted of mice not administered MSC. Hematoxylin and eosin staining was used to determine liver injury. Immunohistochemical analysis was conducted to identify CD34 and vascular endothelial growth factor (VEGF) expression. VEGF gene transcription was detected with RT-PCR. Biochemical analyses were performed to determine alanine aminotransferase, aspartate aminotransferase, total bilirubin,  $\gamma$ -glutamyl transpeptidase, alkaline phosphatase, and albumin levels in serum, and nitric oxide (NO)/nitric oxide synthase (NOS) levels in liver tissues. Transmission electron microscopy was used to observe the ultra-microstructures of hepatocytes.

**Results:** MSC treatment markedly alleviated liver injury and nuclear lesions in the treatment groups compared to the Model group. MSC treatment significantly improved liver functions in the treatment groups compared to the Model group ( $P < 0.05$ ). MSC treatment significantly decreased CD34 expression and NO and NOS levels in liver tissues and suppressed VEGF expression compared to the Model group (all  $P < 0.05$ ).

**Conclusions:** MSC administration alleviated liver injury in a DEN-induced hepatocellular carcinoma rat model through reducing liver enzymes, inhibiting angiogenesis, and suppressing the NO/NOS signaling pathway.

**Keywords:** **Angiogenesis Inhibitors • Carcinoma, Hepatocellular • Drug-Induced Liver Injury • Liver Function Tests**

**Full-text PDF:** <https://www.medscimonit.com/abstract/index/idArt/929255>



## Background

Hepatocellular carcinoma has become the third leading cause of cancer-associated mortality worldwide [1,2]. Surgical resection is the preferred treatment strategy for patients with hepatocellular carcinoma, but recurrence after surgery is common, and the long-term therapeutic effect is not ideal [3,4]. The metastasis of hepatocellular carcinoma through blood and the formation of angiogenesis provide favorable conditions for the invasion of cancer cells [5]. However, because knowledge of hepato-carcinogenesis is still lacking, the therapeutic effects on hepatocellular carcinoma are ineffective, and the clinical prognosis is often poor [6].

Se-methylselenocysteine (MSC), a derivative of selenocysteine methylation, is a natural monomethylated selenoamino acid [7]. MSC is used primarily for anti-aging, selenium supplementation, treatment of cardiovascular/cerebrovascular diseases, and antioxidation [7]. Most importantly, MSC is less toxic than other organic Se compounds or inorganic Se [8]; therefore, the administration of MSC is safe. Previous studies [9,10] have shown that MSC could induce apoptosis and inhibit cell proliferation in prostate cancer, breast cancer, and gastric cancer. However, the preventive effects of MSC on hepatocellular carcinoma have not been clarified.

This study investigated the preventive effects of MSC on oncogenesis in a diethylnitrosamine (DEN)-induced hepatocellular carcinoma rat model and explored the specific mechanisms of MSC.

## Material and Methods

### Animals

A total of 80 Sprague-Dawley rats (Byrness Weil Biotech, Ltd., Chongqing, China), weighing 120 to 150 g, were used for the animal experiments. The rats were randomly divided into a Normal control group (n=16), Model group (n=16), and MSC-treated groups (n=48). Rats in the Normal control group were fed a normal diet (without MSC). Rats in the Model group were fed a normal diet containing 0.1 mg/kg MSC (JK Chem. Beijing, China) 5 times per week for 6 consecutive weeks. Rats in the MSC-treated groups were given 0.3 mg/kg, 1 mg/kg, or 3 mg/kg MSC and assigned as the Model+0.3 mg/kg MSC group, Model+1 mg/kg MSC group, and Model+3 mg/kg MSC group, respectively.

All animal experiments were approved by the Ethics Committee of the Central Hospital of Enshi Tujia and Miao Autonomous Prefecture, Enshi, China. All of the protocols applied in this study were conducted in accordance with the guidelines of the Institutional Animal Care and Use Committee.

### Establishment of the Hepatocellular Carcinoma Rat Model

All model rats (n=64, including the Model, Model+0.3 mg/kg, Model+1 mg/kg, and Model+3 mg/kg MSC groups) were intragastrically administered 100 mg/L of DEN (Shanghai Macklin Biochem Co. Ltd., Shanghai, China) at 1 week after MSC treatment, at a final dosage of 10 mg/kg body weight per day, for consecutive 8 weeks. The rats were then killed at either 2, 4, 8, or 10 weeks, and the liver tumors were studied.

### Hematoxylin and Eosin Staining and Immunohistochemical Assay

The liver samples were isolated and dehydrated using ethanol, cleared using xylene, embedded in paraffin, and sectioned at a thickness of 5  $\mu$ m. The tissue sections were divided into 2 parts: 1 part for hematoxylin and eosin (H&E) staining and 1 part for immunohistochemical assay. For H&E staining, the tissue sections were stained with hematoxylin (Nanjing Jiancheng Bioengineering Institute, Nanjing, China) and eosin (Beyotime Biotech. Shanghai, China) directly. For the immunohistochemical analysis, the tissue sections were de-paraffinized, rehydrated, and heated at 100°C for 10 min to retrieve antigens. Then, the tissue sections were treated using 0.3% hydrogen peroxide to block the endogenous peroxidase and were incubated using goat serum (Hyclone, Logan, UT, USA) for 30 min to block nonspecific binding. The tissue sections were then incubated with rabbit anti-rat CD34 monoclonal antibody (Cat. No. ab81289, 1: 3000, Abcam, Cambridge, MA, USA) and rabbit anti-rat vascular endothelial growth factor (VEGF) polyclonal antibody (Cat. No. ab231260, 1: 2000, Abcam) at 4°C overnight and then incubated using horseradish peroxidase-conjugated goat anti-rabbit IgG (Cat. No. ab6721, 1: 1000, Abcam) for 30 min at room temperature. Finally, the bound secondary antibody was visualized using a diaminobenzidine substrate kit (ZSGB Bio. Co. Ltd., Beijing, China).

### Biochemical Analyses

Blood samples were collected from the rats at 4, 8, and 10 weeks after modeling. To identify the liver functions, the serum levels of alanine aminotransferase (ALT), aspartate aminotransferase (AST), total bilirubin (TBIL),  $\gamma$ -glutamyl transpeptidase (GGT), alkaline phosphatase, and albumin (ALB) were measured using the associated commercial kits, according to the manufacturer's instructions (Nanjing Jiancheng Bioengineering Institute). In addition, the concentrations of nitric oxide (NO) and nitric oxide synthase (NOS) in liver homogenates were determined using an NO assay kit (Cat. No. A012-1-2, Nanjing Jiancheng Bioengineering Institute) and a total NOS assay kit (Cat. No. A014-2-2, Nanjing Jiancheng Bioengineering Institute), according to the manufacturer's instructions.

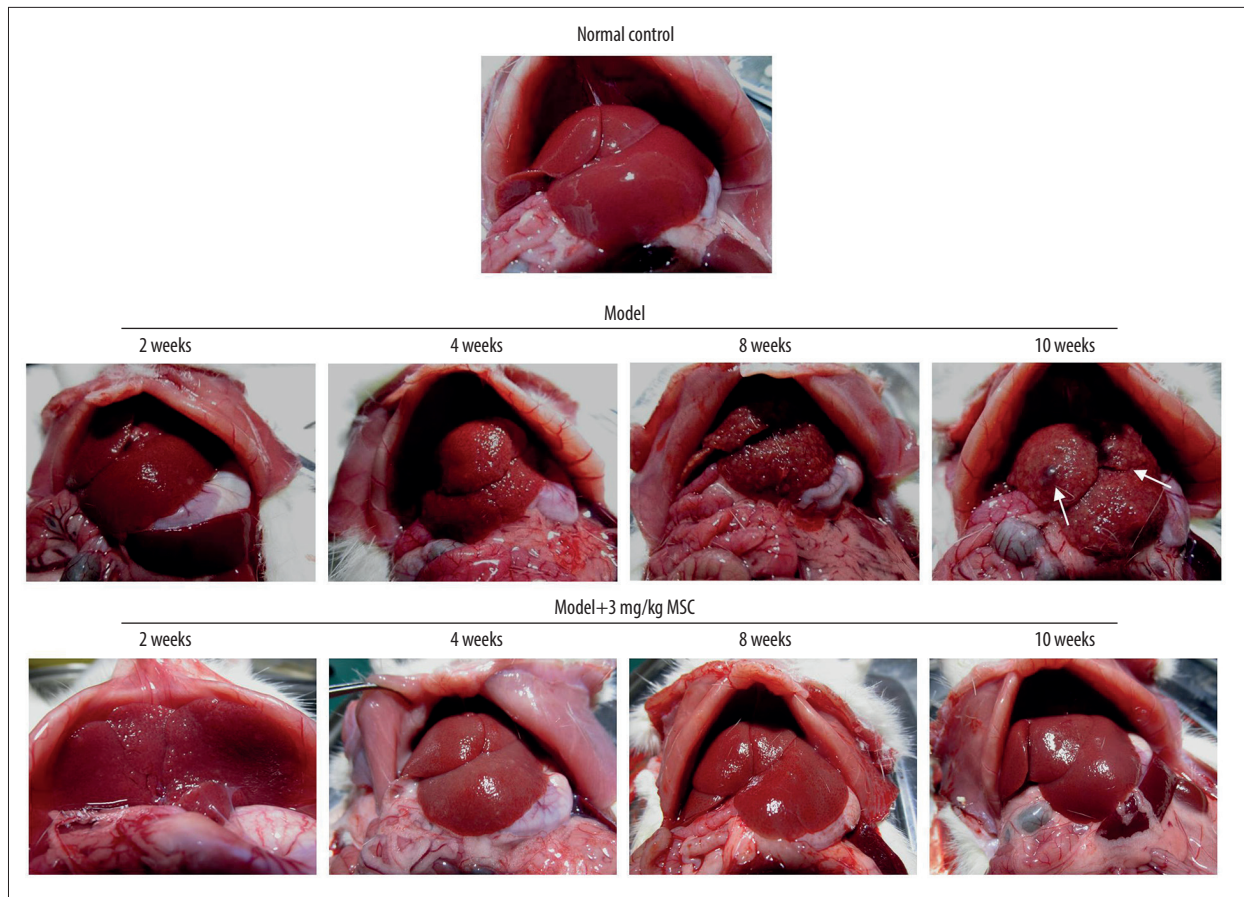


**Figure 1.** Images of liver tissues from hepatocellular carcinoma rat model and model that received 3 mg/kg se-methylselenocysteine (MSC) treatment at 2, 4, 8, and 10 weeks after treatment. The white arrows represent the tumor tissues.

### Transmission Electron Microscopy

The ultra-microstructures and morphology of cells in the liver tissues were determined using transmission electron microscopy (TEM). The liver tissues were collected at 60 min after the reperfusion of the portal venous. Also, the tissue samples were prepared for TEM examination using JEOL JEM-1400PLUS TEM, as described in a previous study [11].

### Reverse Transcription-Polymerase Chain Reaction Assay

Total RNAs of liver tissues were extracted with Trizol reagent (Takara Bio. Dalian, China) and then used to synthesize the complementary DNAs (cDNAs) using a cDNA reverse transcription-polymerase chain reaction (RT-PCR) kit (Western Biotech., Chongqing, China), as instructed by the manufacturer. The specific primers targeting the VEGF gene (sense: 5'-TTCGAGGAAAGGGAAGGGT-3', antisense: 5'-TTAACTCAAGCTGCCTCGCC-3') and the GAPDH gene (sense: 5'-GCCAGC ACCAATAGTTGAACATG-3', antisense: 5'-GAATTGAAGACCCAGAAATGA ACC-3')

were synthesized and used for the RT-PCR assay. The RT-PCR assay was conducted in 96-well plates using a Sybr Green I PCR kit (Western Biotech) with an ABI StepOnePlus PCR system (Foster City, CA, USA). The RT-PCR conditions were as follows: incubation for 4 min at 95°C initially, followed by 40 cycles with incubation for 15 s at 95°C, 1 min at 60°C, and 1 min at 72°C, and termination for 10 min at 72°C. Finally, gene transcription of VEGF was analyzed via normalizing to the GAPDH gene and calculated with the formula of  $2^{-\Delta\Delta Ct}$ , as previously described [12].

### Statistical Analysis

SPSS version 20.0 (IBM Corp., Armonk, NY, USA) was used to analyze the data in this study. ANOVA and Tukey's post hoc test were applied to analyze the differences among groups. Data were represented as the mean±standard deviation. A value of  $P<0.05$  was defined as statistically significant.

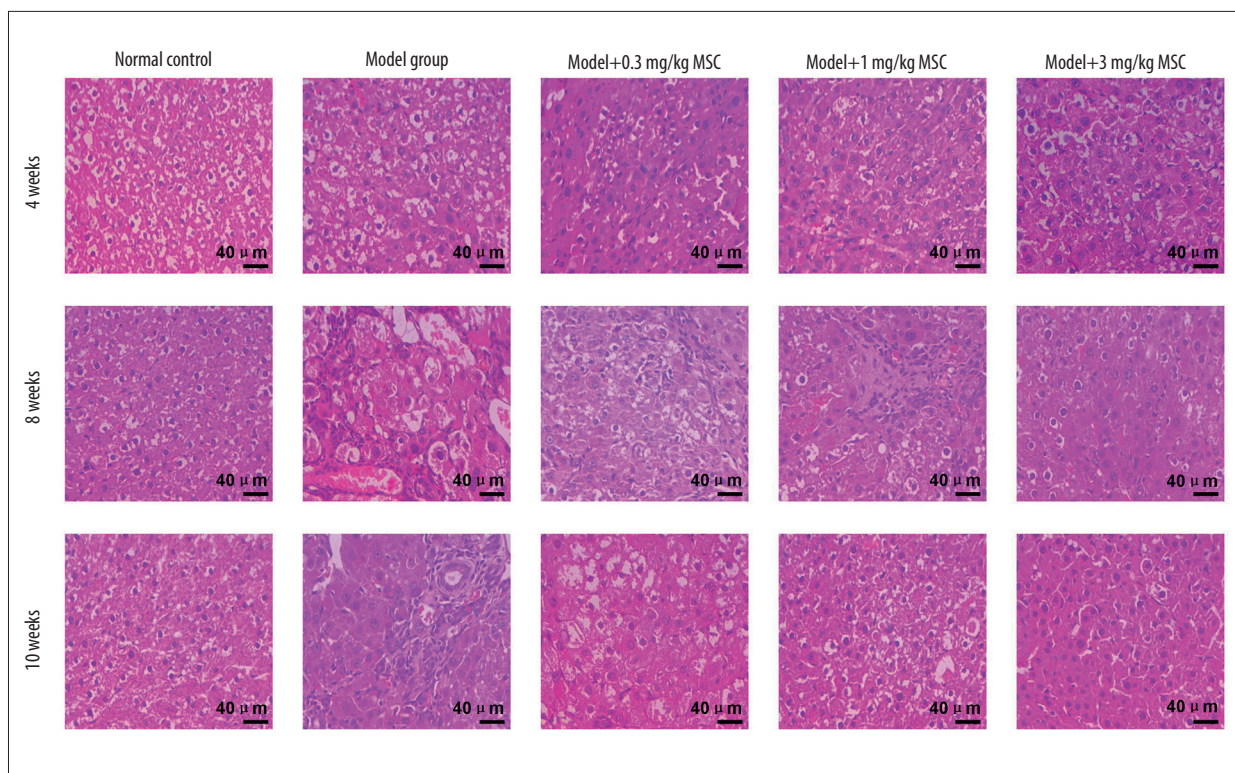


**Figure 2.** Se-methylselenocysteine (MSC) treatment influenced the liver injury of the hepatocellular carcinoma rat model. Liver injury was determined using hematoxylin and eosin staining. The scale bars of 200  $\mu\text{m}$  are illustrated in the images.

## Results

### Hepatocellular Carcinoma Rat Model Was Successfully Created

In the Normal control group, there were no carcinoma nodules on the surface of the rat livers (**Figure 1**). In week 2, the surface of the liver was slightly rough, forming tiny carcinoma nodules (**Figure 1**). In weeks 4 and 8, more gray-white and differently sized carcinoma nodules could be observed (**Figure 1**). In week 10, the liver surface demonstrated obvious tumor lesions (**Figure 1**). These findings demonstrated that the hepatocellular carcinoma rat model was successfully generated.

### MSC Treatment Alleviated Liver Injury of the Rat Model

As shown in **Figure 1**, at 2 weeks after treatment with 3 mg/kg MSC, the liver surface was smooth, with only a few tiny carcinoma nodules (**Figure 1**). While at 4, 8, and 10 weeks after treatment with 3 mg/kg MSC, the liver surface was as smooth as that in the Normal control group, with no carcinoma nodules found on the liver surface (**Figure 1**). Therefore, these results demonstrated that the MSC treatment alleviated the liver injury. However, the experimental results showed that, compared with the Normal control group, the level of liver injury in the Model, Model+0.3, Model+1, and Model+3 mg/kg MSC

groups gradually increased, with the gradual aggravation of the fatty degeneration of the liver and gradual appearance of fibrous tissue proliferation and inflammatory cells, increasing with the length of modeling time of the different rat models (from 4 to 10 weeks) (**Figure 2**). Rats in the Model group demonstrated the most serious pathological changes of liver tissues (**Figure 2**). Compared with the severity of liver injury of rats in the Model group, the severity of liver tissue injury was gradually alleviated with the increased concentrations of MSC (**Figure 2**).

### MSC Treatment Improved Liver Functions of Hepatocellular Carcinoma Rat Model

To show how MSC alleviated hepatocellular carcinoma and improved liver functions, serum levels of ALT, AST, TBIL, GGT, ALP, and TB were measured at weeks 4, 8, and 10. The AST (**Figure 3A**) and ALT (**Figure 3B**) levels were significantly increased in the Model group compared with those in the Normal control group ( $P < 0.01$ ). Compared with the AST (**Figure 3A**) and ALT (**Figure 3B**) levels in the Model group, there were remarkably lower serum levels of AST (**Figure 3A**) and ALT (**Figure 3B**) in the 3 MSC-treated Model groups (0.3 mg/kg, 1 mg/kg, and 3 mg/kg MSC) in a time-dependent manner, gradually decreasing from week 4 to week 10.

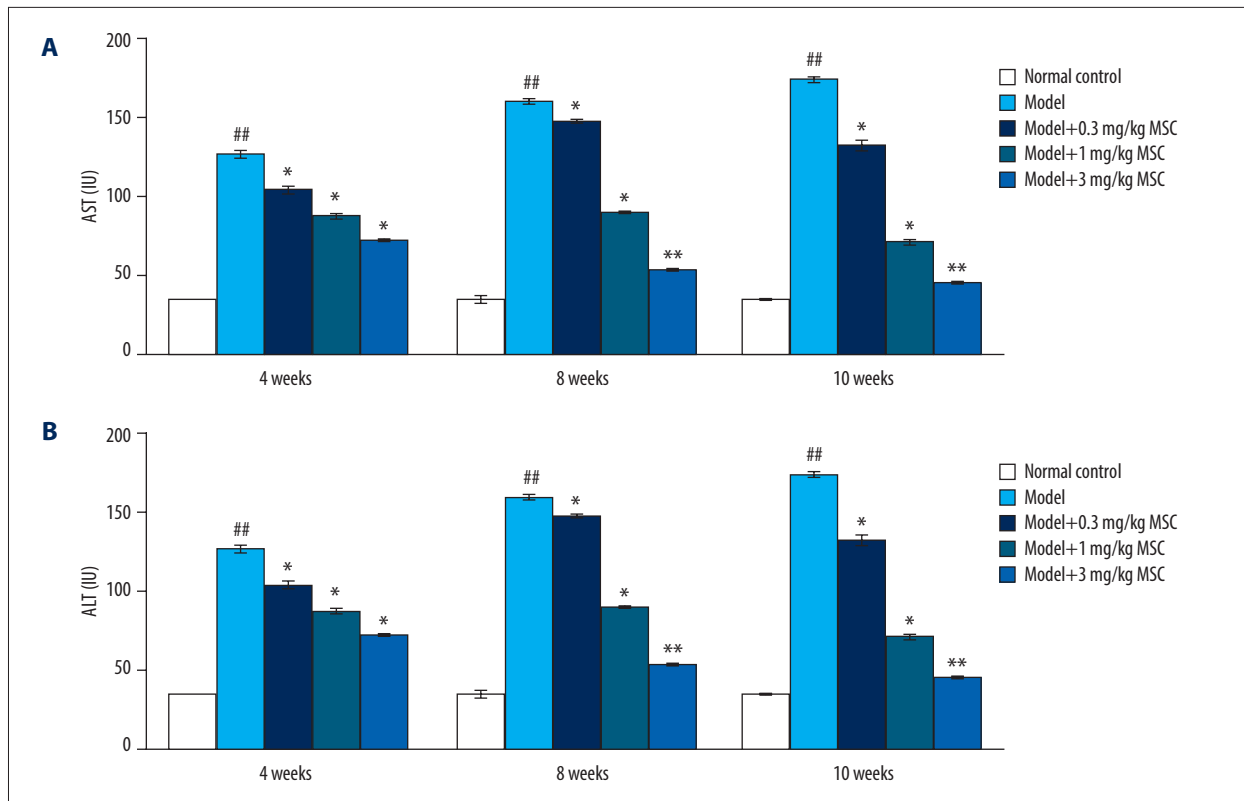


**Figure 3.** Effects of se-methylselenocysteine (MSC) treatments on the liver enzymes, including (A) aspartate aminotransferase and (B) alanine aminotransferase in the serum of rats in different groups. ##  $P<0.01$  vs Normal control group. \*  $P<0.05$  and \*\*  $P<0.01$  vs Model group.

Moreover, the TBIL levels (Figure 4A), ALP activity (Figure 4B), and GGT activity (Figure 4C) in the 3 MSC-treated Model groups were also significantly decreased compared with those in the Model group, also in a time-dependent manner, decreasing from week 4 to week 10. However, the ALB activity (Figure 4D) was markedly increased in the 3 MSC-treated Model groups compared with that of the Model group ( $P<0.05$ ) in a time-dependent manner. Of the 3 MSC treatments, the 3 mg/kg MSC treatment demonstrated the most obvious effects on AST, ALT, TBIL, ALP, GGT, and ALB levels or activity.

#### MSC Treatment Decreased Microvessel Density of the Rat Model

Expression of the endothelial cell biomarker CD34 can reflect the microvessel density (MVD) in tissues. Our findings identified that amounts of CD34-positive cells were significantly increased in the liver tissues of rats in the Model group, compared with those in the Normal control group (Figure 5), at 4, 8, and 10 weeks after modeling. However, the 3 MSC treatments (0.3 mg/kg, 1 mg/kg, and 3 mg/kg MSC) remarkably decreased the amounts of CD34-positive cells in liver tissues of rats, compared with those in the Model group, at 4, 8, and 10 weeks after modeling (Figure 5). The effects of MSC treatment

were also exhibited in a dose-dependent manner, with a gradual decrease with 0.3 mg/kg, 1 mg/kg, 3 mg/kg of MSC. Therefore, we found that MSC treatment could decrease MVD.

#### MSC Treatment Suppressed VEGF Expression in Liver Tissues of the Rat Model

The results showed that VEGF expression in liver tissues of rats in the Model group was significantly higher than that of the Normal control group (Figure 6A). Further, the VEGF expression in the Model group also occurred in a time-dependent manner, gradually increasing from week 4 to week 10 (Figure 6A). The VEGF expression in liver tissues of rats in the Model+0.3 mg/kg MSC, Model+1 mg/kg MSC, and Model+3 mg/kg MSC treatment groups was remarkably suppressed, compared with that in the Model group, at 4, 8, and 10 weeks after modeling (Figure 6A). The effects of MSC treatment also occurred in a dose-dependent manner, gradually decreasing with increasing amounts of MSC.

Furthermore, gene transcription of VEGF in liver tissues of rats in the Model group was significantly higher than that in the Normal control group at 10 weeks after modeling (Figure 6B,  $P<0.05$ ). However, the gene transcription of VEGF in the liver

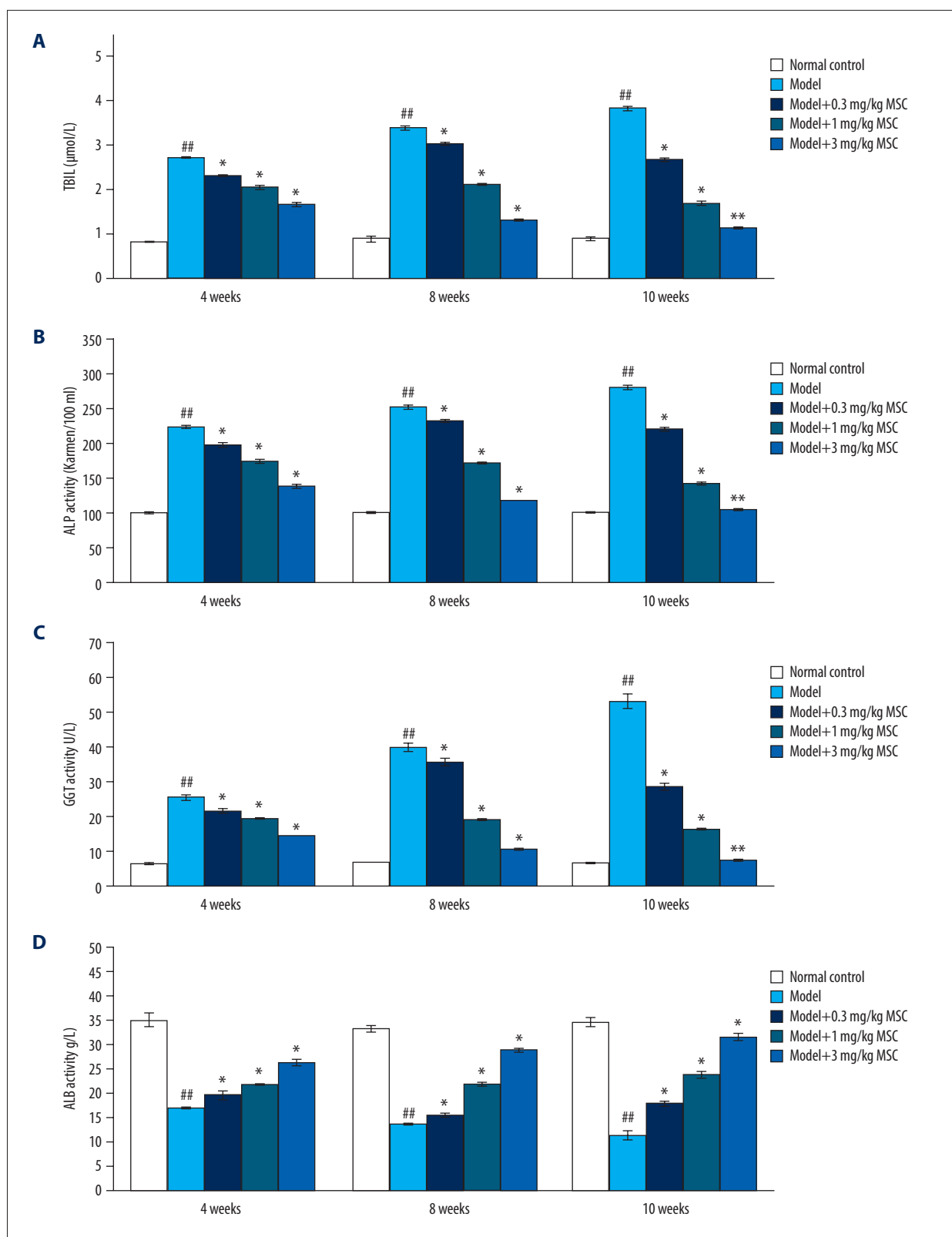


**Figure 4.** Se-methylselenocysteine (MSC) treatments improved liver functions by modulating levels of (A) total bilirubin, (B) alkaline phosphatase, (C)  $\gamma$ -glutamyl transpeptidase, and (D) albumin in serum of rats in different groups. ##  $P < 0.01$  vs Normal control group. \*  $P < 0.05$  and \*\*  $P < 0.01$  vs Model group.

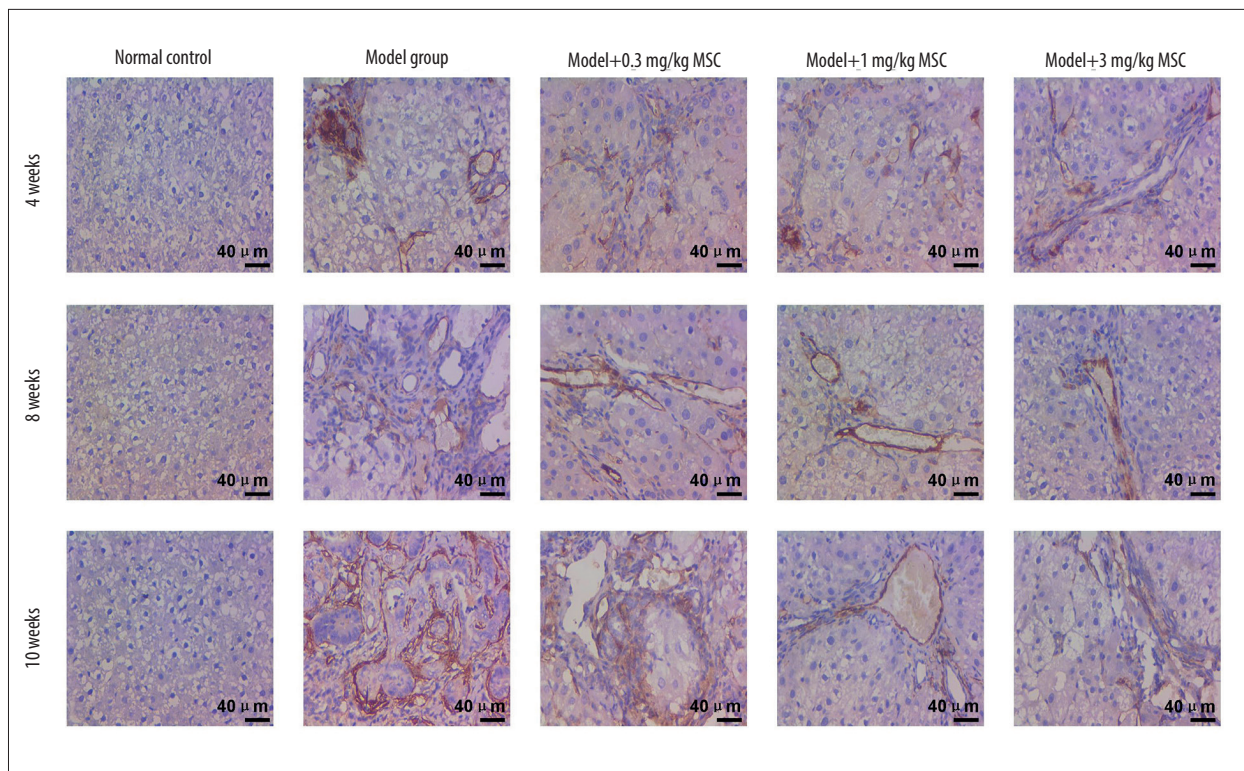


**Figure 5.** Immunohistochemical analysis evaluating the CD34 expression in liver tissues of rats in different groups. The scale bars of 200  $\mu\text{m}$  are illustrated in images.

tissues of rats was markedly suppressed in all 3 MSC treatments (0.3 mg/kg, 1 mg/kg, and 3 mg/kg MSC) compared to that in the Model group (Figure 6B, all  $P < 0.05$ ). The MSC-triggered decrease of VEGF gene transcription also occurred in a dose-dependent manner, gradually decreasing with 0.3 mg/kg, 1 mg/kg, and 3 mg/kg of MSC treatment (Figure 6B).

#### MSC Treatment Alleviated Nuclear Lesions in the Rat Model

Our findings showed that the nuclei of hepatocytes in the Normal control group were round, the nuclear membranes were smooth and clear, and the nuclear spaces were uniform (Figure 7). Also, there were abundant and normal morphological mitochondria and rough endoplasmic reticulum in the cytoplasm (Figure 7). However, in the Model group, the nuclei of the hepatocytes were large and deformed, the shape of the nuclei was irregular, the heterochromatin was significantly increased, the mitochondria were edematous, the rough endoplasmic reticulum was expanded, and the glycogen granules were smaller (Figure 7). Also, some liver cells were necrotic and demonstrated obvious vacuoles in the cytoplasm of the rats in the Model group (Figure 7). The 3 MSC treatments (0.3 mg/kg, 1 mg/kg, and 3 mg/kg MSC) obviously alleviated the nuclear lesions and weakened the pathological degree of hepatocytes gradually, compared to those of rats in the Model

group (Figure 7). We also found that the effects of MSC on nuclear lesions was exhibited in a dose-dependent manner.

#### MSC Treatment Reduced Levels of NO and NOS in the Rat Model

Our results showed that the NO levels (Figure 8A) and NOS levels (Figure 8B) in liver tissues of rats in the Model group were significantly higher than those in the Normal control group (both  $P < 0.05$ ). However, the 3 MSC treatments (0.3 mg/kg, 1 mg/kg, and 3 mg/kg MSC) significantly reduced the NO levels (Figure 8A) and NOS levels (Figure 8B) in liver tissues, compared to the levels in the Model group (all  $P < 0.05$ ). Moreover, the MSC treatment showed an inhibitive effect on NO and NOS levels in a dose-dependent manner.

#### Discussion

MSC is an organic selenium compound, and its toxicity is lower than that of other forms of organic selenium or inorganic selenium [13]. Previous studies [14,15] have shown that MSC can inhibit the growth of a variety of tumor cells, which may be related to its inhibition of neovascularization and induction of apoptosis. To the best of our knowledge, the present study might be the first to pre-administer MSC in a DEN-induced

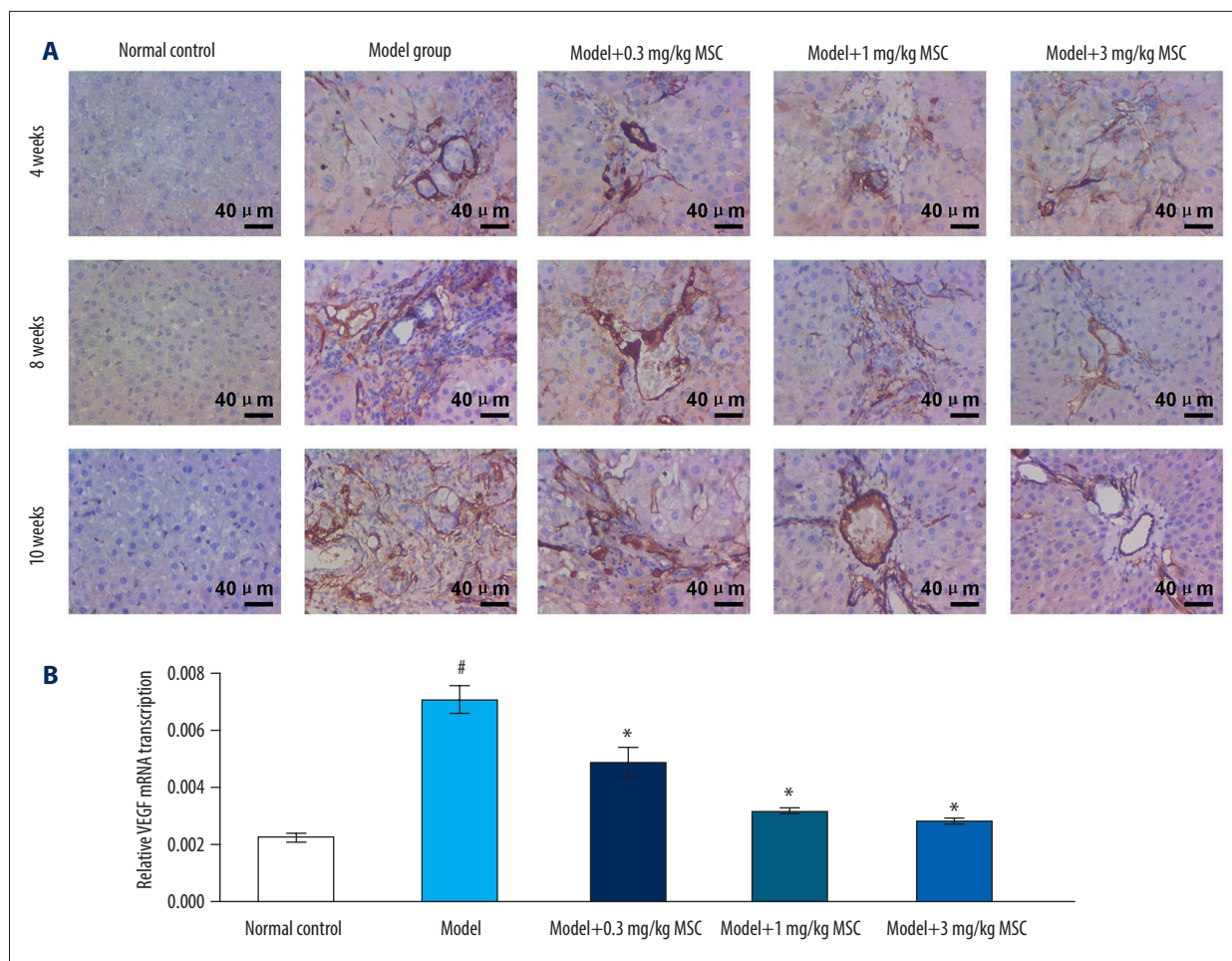


**Figure 6.** Effects of se-methylselenocysteine (MSC) treatments on vascular endothelial growth factor (VEGF) expression in liver tissues of rats in different groups. **(A)** Immunohistochemical analysis for evaluating VEGF expression. The scale bars of 200  $\mu\text{m}$  are illustrated in images. **(B)** RT-PCR assay for assessing VEGF gene transcription. <sup>#</sup>  $P < 0.05$  vs Normal control group. <sup>\*</sup>  $P < 0.05$  vs Model group.

hepatocellular carcinoma rat model and show an alleviated effect on liver injury, improved liver function, decreased VEGF expression, and suppressed formation of MVD.

In the present research, we generated a hepatocellular carcinoma rat model induced by the administration of DEN, which resulted in multiple stages of tumor progression. In weeks 4 and 8, more gray-white and differently sized carcinoma nodules could be observed, while the rat livers had obvious tumor tissues in week 10. These findings show that the hepatocellular carcinoma rat model was successfully generated. In this study, we administered different dosages of MSC in the hepatocellular carcinoma rat model, including 0.3 mg/kg, 1 mg/kg, and 3 mg/kg MSC. H&E staining results showed the gradual aggravation of fatty degeneration of liver and gradual appearance of fibrous tissue proliferation and inflammatory cells, which increased with the modeling time of the models from week 4 to week 10. Compared with the severity of the liver injury of rats

in the Model group, the severity of liver tissues was gradually alleviated with increased concentrations of MSC. Therefore, MSC treatment alleviated liver injury in the rat model.

In our study, the DEN-induced hepatocellular carcinoma rat model also demonstrated hepatic dysfunctions, including the elevation of liver enzymes (AST, ALT, TIBL, and ALP) and cancer biomarker GGT [16] and a decrease in ALB, which are consistent with the findings of El-Maghd et al [17]. The increased levels of AST, ALT, TIBL, and ALP and decreased levels of ALB indicate the injury of hepatocytes and damage in the associated liver functions [18]. Interestingly, the administration of MSC could restore liver functions and reduce hepatocellular carcinoma in rats, which is consistent with the findings of previous studies [19,20], which reported the effects of MSC on hepatocellular carcinoma. Moreover, the effects of MSC treatments on modulating liver enzymes was dose-dependent at weeks 4, 8, and 10 after modeling of 0.3 mg/kg, 1 mg/kg, and 3 mg/kg MSC treatment.



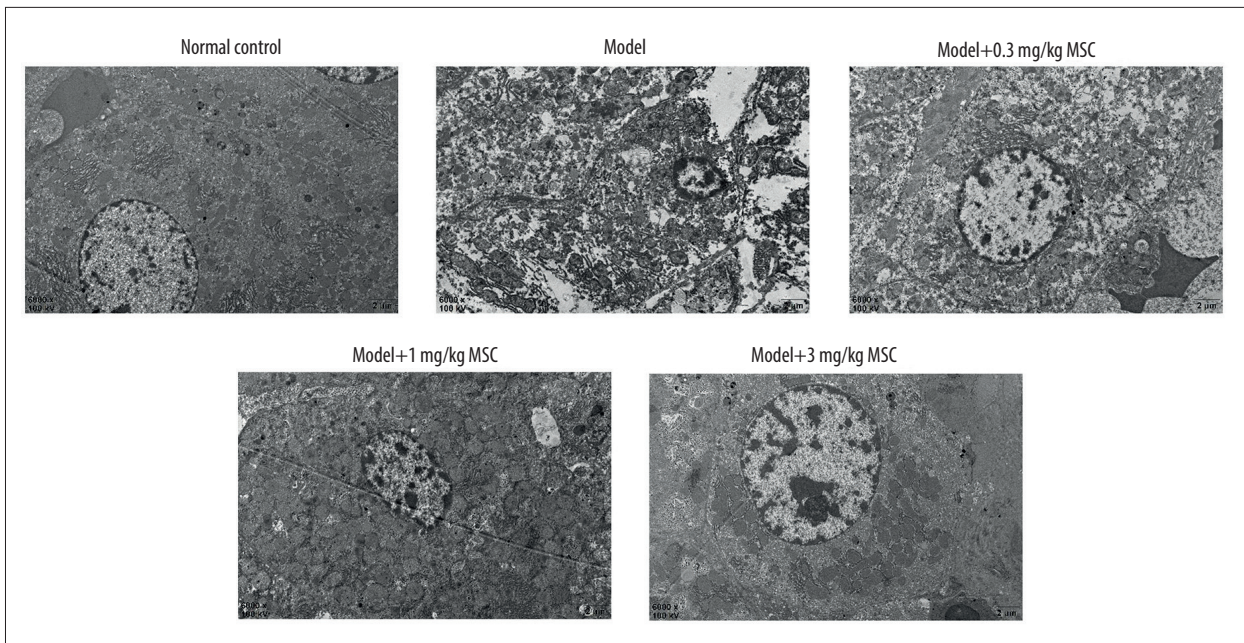


**Figure 7.** Evaluation of ultra-microstructures of hepatocytes in liver tissue using transmission electron microscopy. Magnification 6000 $\times$ .

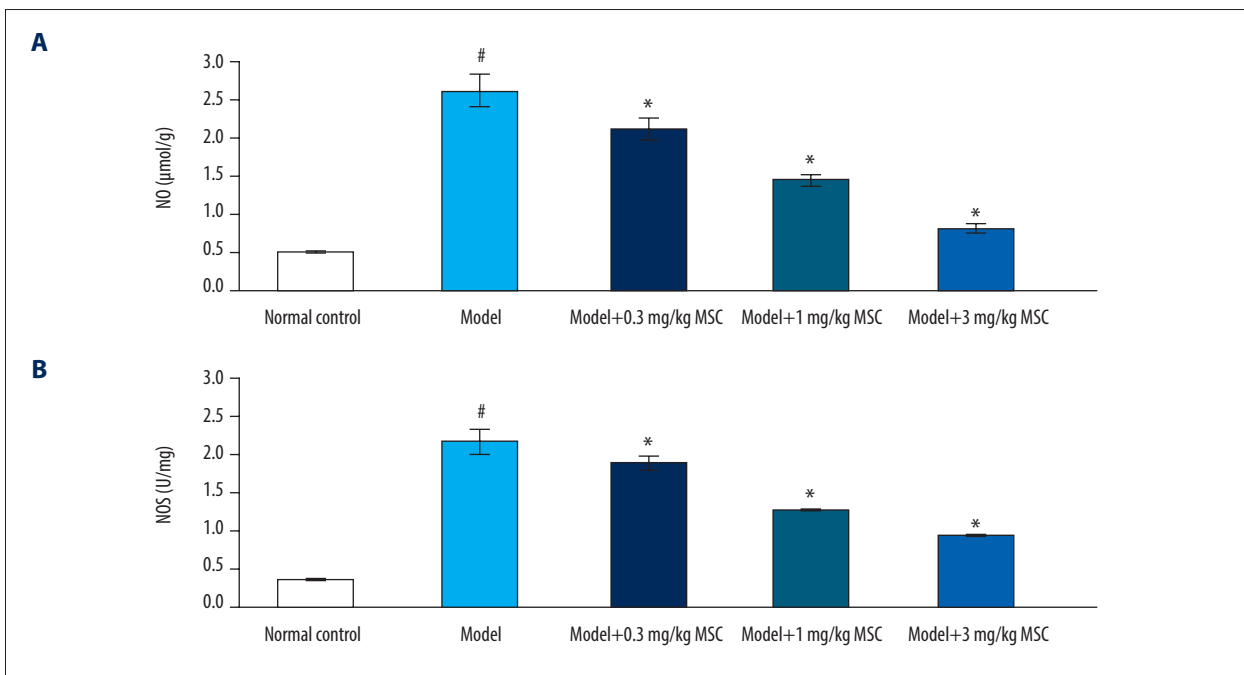


**Figure 8.** Se-methylselenocysteine (MSC) treatments reduced serum levels of nitric oxide (NO) and nitric oxide synthase (NOS) in rats of different groups. **(A)** Statistical analysis of serum NO levels. **(B)** Statistical analysis of serum NOS levels. <sup>#</sup>  $P < 0.05$  vs Normal control group. <sup>\*</sup>  $P < 0.05$  vs Model group.

Hepatocellular carcinoma is a tumor with abundant blood vessels, and neovascularization plays an important role in the progression, metastasis, and invasion of hepatocellular carcinoma [21]. When the diameter of tumor tissues in patients is less than 2 mm, nutrients and oxygen are generally diffused to the surrounding tissues to meet the tumor's growth needs. However, when the diameter of tumor tissue is greater than 2 mm, the dispersed nutrients and oxygen can no longer meet the needs of tumor cell generation, and new blood vessels are needed to provide additional nutrients [22,23]. MVD, as a main index to detect tumor metastasis and growth, can accurately reflect the degree of angiogenesis in patients. Therefore, we evaluated the expression of the CD34 molecule, a biomarker for MVD formation. This study showed that the MVD in the MSC treatment groups was significantly lower in liver tissues, compared to that in the Model group, indicating that MSC treatment can inhibit the formation of new blood vessels. Tumor neovascularization is mainly regulated by angiogenesis inhibitory factors and angiogenesis inducing factors [24]. Among the angiogenic factors, VEGF demonstrates the strongest activity, accelerating the migration and proliferation of endothelial cells and promoting the formation of new blood vessels [25,26]. In this study, VEGF was highly expressed in tumor tissues and overexpressed in the serum of rats in the Model group. Compared with that of the Model group, the expression of VEGF in liver tissues and in the contents of serum in the MSC treatment groups was significantly lower, indicating that MSC inhibited the formation of new blood vessels by inhibiting secretion of the VEGF molecule. Furthermore, MSC treatment triggered the decrease of VEGF gene transcription in a dose-dependent manner.

We also found that a few liver cells were necrotic and demonstrated obvious vacuoles in the cytoplasm of rats in the Model group. However, the above liver cell damage was alleviated by MSC treatment. Thus, the MSC treatments alleviated the nuclear lesions in the rat model, which indirectly improved the

morphology and characteristics of the hepatocytes. Moreover, a previous study [17] reported that MSC treatment could up-regulate the transcription of proapoptotic genes, such as caspase-3 and Bax, in liver tissues of a hepatocellular carcinoma rat model. Other studies [9,10] reported that MSC could suppress the proliferation of cancer cells through inducing caspase activation-mediated apoptosis. However, our present study did not clarify the mechanism of apoptosis in liver tissues of the DEN-induced hepatocellular carcinoma rat model, which is a limitation of our study. In a future study, we would like to examine apoptosis activation in liver tissues of a hepatocellular carcinoma model.

According to the findings of previous studies [27,28], NO and NOS participate in the occurrence and progression of hepatocellular carcinoma and are correlated with its angiogenesis and invasion/metastasis. We identified that NO and NOS levels in liver tissues of the rats in the Model group were remarkably increased, and these levels were inhibited by treatment with MSC. Therefore, the effects of MSC treatment on the progression of hepatocellular carcinoma were also mediated by modulating the NO/NOS signaling pathway [29].

## Conclusions

This study demonstrated that MSC administration could alleviate liver injury and prevent oncogenesis in liver tissues of a DEN-induced hepatocellular carcinoma rat model by reducing liver enzymes, inhibiting angiogenesis, and suppressing the NO/NOS signaling pathway. We believe the preventive strategy of using MSC in this study would be beneficial in patients with hepatocellular carcinoma.

## Conflicts of Interest

None.

## References:

1. Zong C, Zhang H, Yang X, et al. The distinct roles of mesenchymal stem cells in the initial and progressive stage of hepatocarcinoma. *Cell Death Dis.* 2018;9:345
2. He G, Chen Y, Zhu C, et al. Application of plasma circulating cell-free DNA detection to the molecular diagnosis of hepatocellular carcinoma. *Am J Transl Res.* 2019;11:1428-45
3. Klimaszewska M, Górska S, Dawidowski M, et al. Biosynthesis of Se-methylseleno-L-cysteine in *Basidiomycetes* fungus *Lentinula edodes* (Berk.) Pegler. *Springerplus.* 2016;5:733-35
4. Liu B, Liu T, Su M, et al. Improving the surgical effect for primary liver cancer with intraoperative fluorescence navigation compared with intraoperative ultrasound. *Med Sci Monit.* 2019;25:3406-16
5. Zhang Y, Davis C, Shah S, et al. IL-33 promotes growth and liver metastasis of colorectal cancer in mice by remodeling the tumor microenvironment and inducing angiogenesis. *Mol Carcinog.* 2017;56:272-87
6. Yu LX, Yan HX, Liu Q, et al. Endotoxin accumulation prevents carcinogen-induced apoptosis and promotes liver tumorigenesis in rodents. *Hepatology.* 2010;52:1322-33
7. Johnson WD, Morrissey RL, Kapetanovic I, et al. Subchronic toxicity studies of Se-methylselenocysteine, an organoselenium compound for breast cancer prevention. *Food Chem Toxicol.* 2008;46:1068-78
8. El-Bayoumy K, Sinha R. Mechanisms of mammary cancer chemoprevention by organoselenium compounds. *Mutat Res.* 2004;551:181-97
9. Medina D, Thompson H, Ganther H, et al. Se-methylselenocysteine: A new compound for chemoprevention of breast cancer. *Nutr Cancer.* 2001;40:12-17
10. Dalla Corte CL, Ramos A, Dos Santos CM, et al. Selenium and mercury levels in rat liver slices co-treated with diphenyl diselenide and methylmercury. *Biometals.* 2016;29:543-47
11. Yamanaka K, Hatano E, Narita M, et al. Olprinone attenuates excessive shear stress through up-regulation of endothelial nitric oxide synthase in a rat excessive hepatectomy model. *Liver Transpl.* 2011;17:60
12. Livak KJ, Schmittgen TD. Analysis of relative gene expression data using real-time quantitative PCR and the  $2^{-\Delta\Delta Ct}$  method. *Methods.* 2001;25:402-8
13. Fakh M, Cao S, Durrani FA, et al. Selenium protects against toxicity induced by anticancer drugs and augments antitumor activity: A highly selective, new, and novel approach for the treatment of solid tumors. *Clin Colorectal Cancer.* 2005;5:132-35
14. Chakraborty P, Roy SS, Bhattacharya S. Molecular mechanism behind the synergistic activity of diphenylmethyl selenocyanate and cisplatin against murine tumor model. *Anticancer Agents Med Chem.* 2015;15:501-10
15. Bhattacharya A, Toth K, Sen A, et al. Inhibition of colon cancer growth by methylselenocysteine-induced angiogenic chemomodulation is influenced by histologic characteristics of the tumor. *Clin Colorectal Cancer.* 2009;8:155-62
16. Wang Q, Shu X, Dong Y, et al. Tumor and serum gamma-glytamyl transpeptidase, new prognostic and molecular interpretation of an old biomarker in gastric cancer. *Oncotarget.* 2017;8:36171-84
17. El-Magd MA, Mohamed Y, El-Shetry ES, et al. Melatonin maximizes the therapeutic potential of non-preconditioned MSCs in a DEN-induced rat model of HCC. *Biomed Pharmacother.* 2019;114:108732
18. Abdelhady D, El-Abasy M, Abou-Asa S, et al. The ameliorative effect of aspergillus awamori on aflatoxin B1-induced hepatic damage in rabbits. *World Mycotoxin J.* 2017;10:363-73
19. Moreira AJ, Ordóñez R, Cerski CT, et al. Melatonin activates endoplasmic reticulum stress and apoptosis in rats with diethylnitrosamine-induced hepatocarcinogenesis. *PLoS One.* 2015;10:e0144517
20. Mortezaee K, Khanlarkhani N, Sabbaghziarani F, et al. Preconditioning with melatonin improves therapeutic outcomes of bone marrow-derived mesenchymal stem cells in targeting liver fibrosis induced by CCl4. *Cell Tissue Res.* 2017;369:303-12
21. Ren J, Lu Y, Qian Y, et al. Recent progression regarding kaempferol for the treatment of various diseases. *Exp Ther Med.* 2019;18:2759-76
22. Ramjiawan RR, Griffioen AW, Duda DG. Anti-angiogenesis for cancer revisited: Is there a role for combinations with immunotherapy? *Angiogenesis.* 2017;20:185-204
23. Eelen G, de Zeeuw P, Simons M, et al. Endothelial cell metabolism in normal and diseased vasculature. *Circ Res.* 2015;116:1231-44
24. Li RL, Huang JJ, Shi YQ, et al. Pulsed electromagnetic field improves postnatal neovascularization in response to hindlimb ischemia. *Am J Transl Res.* 2015;7:430-44
25. Hoeben A, Landuyt B, Highley MS, et al. Vascular endothelial growth factor and angiogenesis. *Pharmacol Rev.* 2004;56:549-80
26. Sun J, Zhao Z, Zhang W, et al. Spalt-like protein 4 (SALL4) promotes angiogenesis by activating vascular endothelial growth factor A (VEGFA) signaling. *Med Sci Monit.* 2020;26:e920851
27. Wang R, Geller DA, Wink DA, et al. NO and hepatocellular cancer. *Pharmacol.* 2019;18:14838
28. Yu DC, Chen J, Sun XT, et al. Mechanism of endothelial progenitor cell recruitment into neo-vessels in adjacent non-tumor tissues in hepatocellular carcinoma. *BMC Cancer.* 2010;10:435
29. Cui Y, Zhang Y, Liu G. Syringin may exert sleep-potentiating effects through the NOS/NO pathway. *Fundam Clin Pharmacol.* 2015;29:178-84